ACS APPLIED MATERIALS & INTERFACES

Research Article

www.acsami.org

Effect of PEDOT Nanofibril Networks on the Conductivity, Flexibility, and Coatability of PEDOT:PSS Films

Jin Young Oh,[†] Minkwan Shin,[†] Jae Bok Lee,[‡] Jong-Hyun Ahn,[‡] Hong Koo Baik,*[,†] and Unyong Jeong*[,†]

[†]Department of Materials Science and Engineering and [‡]Department of Electrical and Electronic Engineering, Yonsei University, 134 Shinchon-dong, Seoul, Korea

Supporting Information

ABSTRACT: The use of poly(3,4-ethylenedioxythiophene):poly(styrenesulfonate) (PEDOT:PSS) in electrodes and electrical circuits presents a number of challenges that are yet to be overcome, foremost amongst which are its relatively low conductivity, low coatability on hydrophobic substrates, and decreased conductivity at large strains. With this in mind, this study suggests a simple way to simultaneously address all of these issues through the addition of a small amount of a nonionic surfactant (Triton X-100) to commercial PEDOT:PSS solutions. This surfactant is shown to considerably reduce the surface tension of the PEDOT:PSS solution, thus permitting conformal coatings of PEDOT:PSS thin film on a diverse range of hydrophobic substrates. Furthermore, this surfactant induces the formation of PEDOT nanofibrils during coating, which led to the high conductivity values and mechanical stability at large strains (ε = 10.3%). Taking advantage of the superior characteristics of these PEDOT:PSS thin films, a highly flexible polymer solar cell was fabricated. The power conversion efficiency of this solar cell (3.14% at zero strain) was preserved at large strains (ε =7.0%).

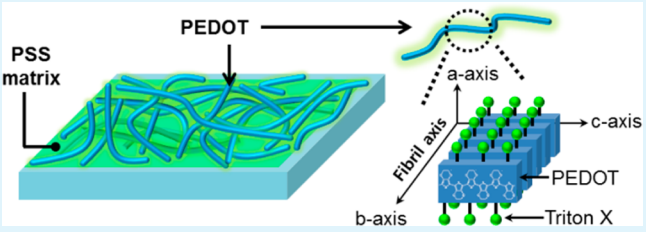

KEYWORDS: *conducting polymer, PEDOT:PSS, nanofibril, flexibility, wettability, organic solar cell*

INTRODUCTION

Conductive polymers have been widely investigated as a potential new type of flexible transparent electrode. Of these, particular interest has been given to poly(3,4-ethylenedioxythiophene):poly(styrenesulfonate) (PEDOT:PSS) because the aqueous solution used for its coating is environmentally friendly and its electrical properties are relatively stable in ambient air.[1] At present, PEDOT:PSS aqueous solutions are commercialized under trade names of Baytron, Clevios, Orgacon, etc., with many different formulations available offering a range of viscosities and conductivities. These products have been investigated as potential replacements for brittle indium−tin oxide (ITO) electrodes[2,3] and have already been widely used as a hole-transporting layer in optoelectronic devices because of the fact that their high work function facilitates the injection/extraction of holes.[4]

Nevertheless, there are a number of challenges that need to be overcome before PEDOT:PSS can be extensively used in commercially produced electrodes and electric circuits, among which are its relatively low conductivity, low coatability on hydrophobic substrates, reduced conductivity at large strains, and instability of its conductance when exposed to humidity.[5−10] Furthermore, from a practical perspective, all of these challenges need to be addressed simultaneously. It is already known that the effect of humidity can be mitigated to some degree by using a barrier layer to block the penetration of oxygen and water molecules.[11,12] The low conductivity of pristine PEDOT:PSS has been improved by the addition of organic compounds such as dimethyl sulfoxide (DMSO),[13] ethylene glycol (EG),[14,15] diethylene glycol,[16] and sorbitol.[17] Such chemical treatments have been discussed in detail in a review by Po et al.[18] The highest conductivity (~1000 S/cm) was obtained by the addition of DMSO or EG to pristine solutions.[13−15] The conductivity has also been enhanced to over 4000 S/cm by treating the film with sulfuric acid,[19,20] but the use of this hazardous chemical process is not desirable for commercial device fabrication.

Unfortunately, these aqueous solutions of PEDOT:PSS and polar compounds cannot be coated onto hydrophobic substrates. A PEDOT film with excellent conductivity can be coated on a hydrophobic surface via vapor-phase polymerization;[21] however, this approach does not take full advantage of the direct printing of PEDOT:PSS. Consequently, a nonionic fluorosurfactant polymer (Zonyl) has been used to improve the wetting of PEDOT:PSS solutions.[16,22] Bao et al. recently reported that a small fraction of Zonyl (0.1 wt %) has a synergistic effect with DMSO in enhancing the conductivity of PEDOT:PSS.[23] In this way, they succeeded in preparing a highly conductive PEDOT:PSS thin film (42 Ω/□ at 82% transparency) on a hydrophobic poly(dimethylsiloxane) (PDMS) substrate. The stability of a PEDOT:PSS thin film's

Received: February 5, 2014
Accepted: April 8, 2014
Published: April 8, 2014

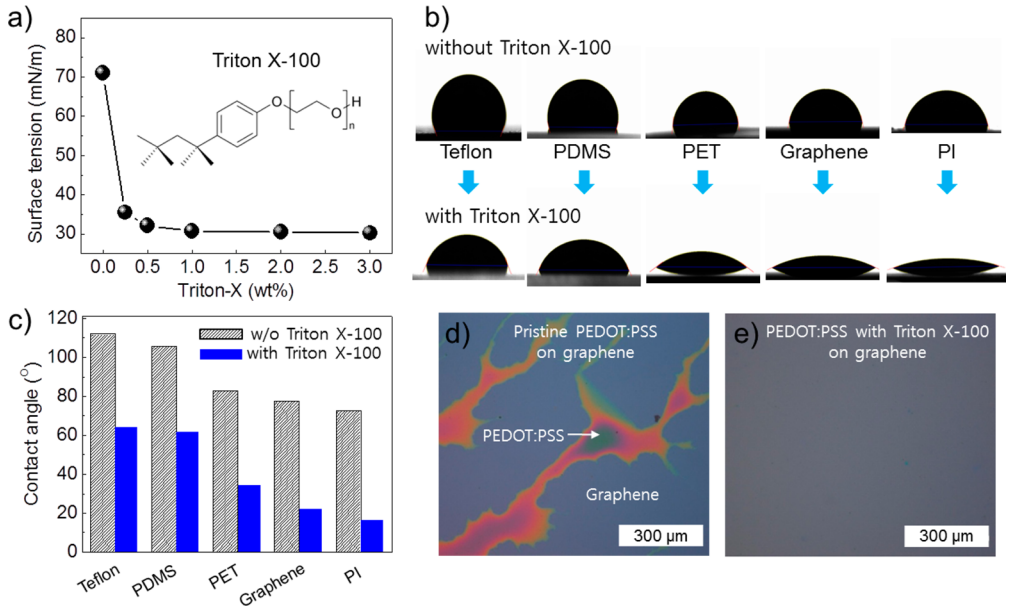

Figure 1. (a) Surface tension of a PEDOT:PSS solution (Clevios P) as a function of the surfactant (Triton X-100) concentration (wt %) versus the total amount of PEDOT:PSS. (b) Optical microscopy images of PEDOT:PSS solutions without/with the surfactant (1 wt %) on different hydrophobic substrates. (c) Change in the contact angle without/with the surfactant (1 wt %). (d and e) Optical microscopy images obtained from PEDOT:PSS solutions spin-coated without (d) and with (e) the surfactant onto graphene surfaces.

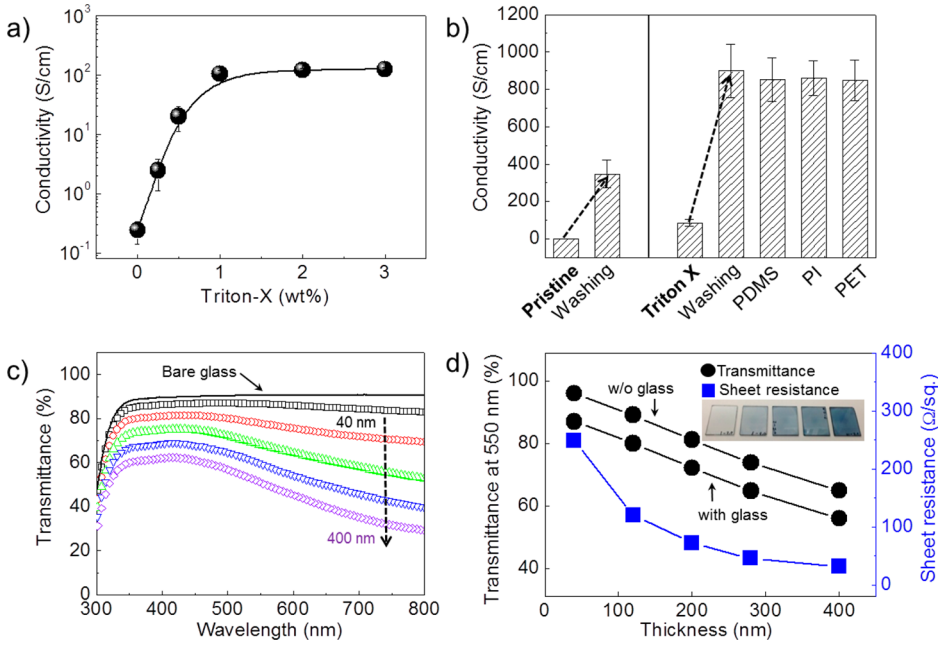

Figure 2. (a) Conductivity of the PEDOT:PSS films on glass as a function of the surfactant weight fraction (f_{surf} = 100 (wt %) × $W_{surfactant}$/$W_{PEDOT:PSS}$). (b) Conductivity of the PEDOT:PSS films before and after washing the PSS phase with methanol. (c) Transparency of the PEDOT:PSS films in relation to their thickness. (d) Transmittance (left axis, circle symbol) of a film with a surfactant (f_{surf} = 1.0 wt %) at 550 nm and its sheet resistance (right axis, square symbol).

conductivity under different bending strains has also been investigated, revealing that the highly conductive films obtained by adding polar solvents (EG or DMSO) experience considerable degradation in conductivity at large strains (>2%). This electrical instability at large strains, which is not observed in metallic electrodes,[24,25] is attributed to the increased modulus of the film, followed by evaporation of the solvent. Thus, a simple approach that can address all of the issues associated with PEDOT:PSS thin films is urgently needed.

Although the exact reason for the enhanced conductivity in the presence of additives still warrants further investigation, it is clear that any PEDOT microphase should interconnect to form a bicontinuous structure with the PSS phase.[26] From percolation theory, one-dimensional conductive fillers are known to have a lower threshold volume fraction for percolation than granular or spherical fillers.[27,28] Furthermore, with respect to flexibility, it has been proven that the electrical properties of a thin film formed by conductive nanofibrils are preserved under extreme strain situations such as during folding

and stretching.[29−31] Therefore, a network structure that incorporates nanofibril PEDOT microphases is clearly desirable in terms of achieving both high conductivity and extreme flexibility.

In this study, a small-molecule nonionic surfactant (Triton X-100) was added to a PEDOT:PSS solution in order to facilitate the deposition of PEDOT:PSS nanofibril thin films onto hydrophobic substrates. The conductivity, electrical stability on mechanical bending, and coatability of these films are discussed herein. Also, flexible polymer solar cells incorporating the film were assessed with a view to their practical application.

RESULTS AND DISCUSSION

Figure 1a shows the change in the surface tension of the PEDOT:PSS solution as a function of the Triton X-100 concentration (chemical structure shown in the inset) in the pristine solution (Clevios P). The solid content of the pristine solution was 1.3 wt %, and the ratio of PEDOT to PSS was 1:2.5 by weight. The surfactant was mixed in the pristine solution so that the weight fraction (f_{surf}) of the surfactant versus the PEDOT:PSS solute [f_{surf} = 100 (wt %) × W_{surf}/$W_{PEDOT:PSS}$] was 0.25−3.0 wt %. Owing to the high surface tension of the pristine PEDOT:PSS solution (71.03 mN/m), which is similar to that of pure water (71.97 mN/m), the pristine solution was readily dewetted on hydrophobic surfaces. However, the surface tension of the PEDOT:PSS solution was markedly reduced to 35 mN/m at f_{surf} = 0.25 wt % and saturated (30.8 mN/m) at f_{surf} = 1.0 wt %. As shown in Figure 1b, this decrease in the surface tension has the effect of reducing the contact angle of the PEDOT:PSS solution on a variety of frequently used hydrophobic surfaces, including poly(tetrafluoroethylene) (Teflon), PDMS, poly(ethylene terephthalate) (PET), graphene, and polyimide (PI). The concentration of the surfactant was fixed at f_{surf} = 1.0 wt %. The contact angles on the substrates are summarized in Figure 1c. As examples, the contact angle on a Teflon sheet was reduced from 112° to 63°, and the value on a PDMS substrate dropped from 106° to 60°. The reduced contact angle enabled coating of PEDOT:PSS on all of the hydrophobic substrates tested in this study. In the case of PEDOT:PSS spin-coated onto a graphene substrate, the pristine PEDOT:PSS solution readily dewetted, whereas the addition of surfactant created a uniform coating without any obvious signs of dewetting. A similarly uniform coating was readily obtained on the other substrates [see the Supporting Information (SI), Figure S1].

Figure 2a shows the effect of Triton X-100 addition on the conductivity of PEDOT:PSS films coated onto glass substrates. The pristine PEDOT:PSS film yielded a low electrical conductivity (0.24 S/cm), whereas the conductivity of the as-coated films increases sharply as the surfactant concentration was increased to a saturation point (∼100 S/cm) at a surfactant concentration (f_{surf}) of 1.0 wt %. The selective removal of the PSS phase on the surface of the film by methanol drops, while spinning the specimen on a spin coater (typically, 0.5 mL per drop at 3000 rpm) increased the conductivity of the film. The reduced volume allowed the PEDOT microdomains to form an increased number of direct contacts. From the X-ray photoelectron spectroscopy (XPS) S 2p spectra, the atomic percentage of PEDOT on the surface of those films with surfactant increased from 35 to 45% after the film was washed with methanol (see the SI, Figure S2). Moreover, the conductivity of the methanol-washed films (Figure 2b) on a glass substrate showed an increase of up to 347 ± 75 S/cm over a pristine PEDOT:PSS film. More importantly, however, the conductivity of a PEDOT:PSS film with the surfactant (f_{surf} = 1.0 wt %) on a glass substrate was increased to 852 ± 143 S/cm by methanol washing. Similarly, high conductivity values were also obtained on other hydrophobic substrates such as PDMS, PI, and PET.

For comparison, a different PEDOT:PSS product (Clevios PH500) designed for electrode use was evaluated. Figure S3a in the SI shows the electrical conductivity of this PEDOT:PSS film as a function of the surfactant weight fraction. The conductivity of the pristine Clevios PH500 was 0.85 ± 0.08 S/cm, which was only slightly higher than that of Clevios P (0.24 ± 0.1 S/cm). The conductivity of Clevios PH500 also exhibited a sharp increase with the weight fraction of the surfactant, becoming saturated (93.46 ± 8.9 S/cm) at f_{surf} = 1.0 wt % (see the SI, Figure S3a). Methanol washing was also found to increase the conductivity of both the pristine and surfactant-modified films (see the SI, Figure S3b). However, the conductivity of the pristine Clevios PH500 showed a much greater increase after methanol washing (525 ± 40.8 S/cm) than the pristine film of Clevios P (347 ± 75 S/cm). Yet despite this, the conductivity of a Clevios PH500 film with f_{surf} = 1.0 wt % increased to a value (882 ± 75 S/cm) very similar to that of the surfactant-modified Clevios P film (847 ± 109 S/cm). These results indicate that the effect of surfactant addition and methanol washing is not dependent on the specific batch or formulation of the PEDOT:PSS used.

Figure 2c shows transmittance of the PEDOT:PSS films containing Triton X-100 (f_{surf} = 1.0 wt %) with respect to the film thickness. The thickness was controlled by repeated spin coating after the previous PEDOT:PSS layer had dried. In all cases, a very similar relationship between transmittance and thickness was discernible. The 40-nm-thick thin film was highly transparent (96% without glass and 87% with glass) to visible light. Figure 2d shows the sheet resistance as a function of the film thickness at a wavelength of 550 nm, in which the sheet resistance of the 40-nm-thick film was 240 Ω/□ at 96% transmittance (87% with glass) and that of the 400-nm-thick film was 32 Ω/□ at 65% transmittance (55% with glass). These values are the same as those previously obtained by combining DMSO and Zonyl surfactants.[32]

It is worth noting in Figure 3 that the conductivity after washing with alcohol was clearly dependent on the alcohol species. Specifically, as the number of carbons in the alcohol is increased, the solubility of PSS decreases, whereas that of PEDOT increases. Methanol was therefore found to be the most suitable solvent because it dissolved out the PSS phase without disturbing the morphology of the PEDOT phase. As a result, the conductivity achieved by washing with methanol was not sensitive to the extent of the wash. This is confirmed in Figure 4a, which clearly shows that the conductivity was significantly increased after the first drop of methanol, becoming saturated with further droplets. We therefore sought to determine whether the conductivity is dependent on the residence time in alcohol, subsequently finding that immersion times of 2 and 30 min yielded the same conductivity (Figure 4b).

PEDOT:PSS films are known to have a bicontinuous structure that arises as a result of microphase separation during the coating process. Consequently, in order to achieve high conductivity, the PEDOT phase should consist of nanoscale microdomains with a good network structure, sharp interfaces with the PSS phases, and a well-developed crystal structure.

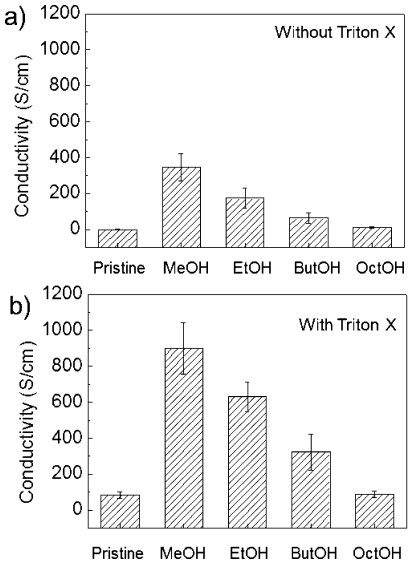

Figure 3. Conductivity of PEDOT:PSS films (a) without and (b) with Triton X-100 after washing with various alcohols (methanol, ethanol, butanol, and octanol in order). Pristine refers to the PEDOT:PSS film before the washing process.

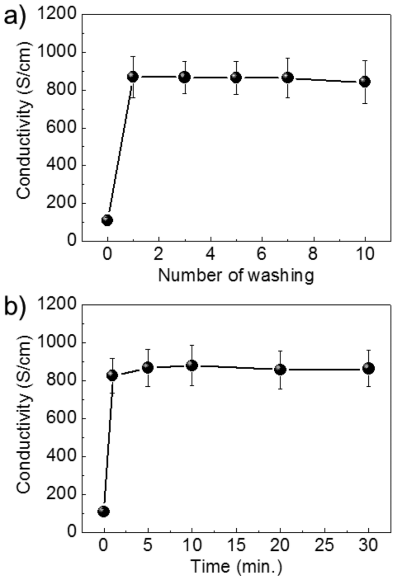

Figure 4. (a) Conductivity of a PEDOT:PSS thin film with surfactant as the thin film was washed with different numbers of methanol drops while it was spun on a spin coater. (b) Conductivity of a PEDOT:PSS thin film with surfactant as a function of the methanol dipping time.

These two latter aspects are inherently linked because a well-developed crystal naturally creates sharp interfaces.[26] The effect of the surfactant on the morphology of the PEDOT phase was therefore investigated by atomic force microscopy (AFM) and transmission electron microscopy (TEM). The PSS phase was partially dissolved with methanol in order to obtain clearer images of the PEDOT phase. The PEDOT phase with surfactant showed a nanofibril structure, while the PEDOT phase without surfactant showed the typical aggregation of nanosized granules. In the TEM images, the darker regions represent areas of greater electron density, in this case correlating with the self-assembled PEDOT phase, which has a greater density than the amorphous phase. The notable difference between the two was that the pristine PEDOT:PSS film contained granular PEDOT phases (Figure 5a,b), whereas

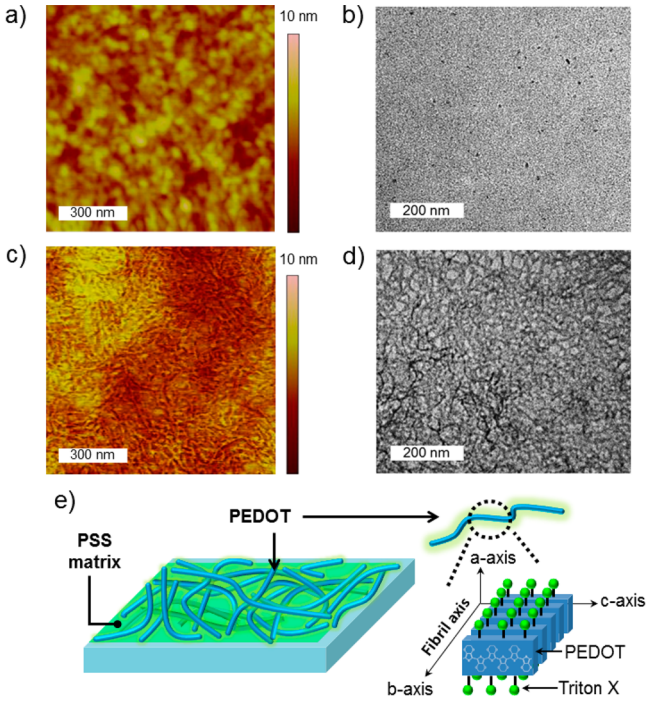

Figure 5. AFM and TEM images of (a and b) a pristine PEDOT:PSS film and (c and d) a PEDOT:PSS film with surfactant (f_{surf} = 1.0 wt %). (e) Schematic illustration of a PEDOT:PSS thin film with surfactant depicting the molecular packing of PEDOT in nanofibrils.

the surfactant-modified films formed a network of nanofibrils (~30 nm wide; Figure 5c,d). AFM phase images of these PEDOT:PSS films are shown in Figure S4 in the SI. The effect of methanol washing on the morphology of PEDOT was checked. AFM and TEM images of the PEDOT phase obtained prior to washing the PSS phase with methanol are provided in Figure S5 in the SI, which shows the same morphologies as those observed in Figure 5. This indicates that formation of the nanofibrils was caused by the surfactant not by methanol washing. Unfortunately, the average length of the nanofibrils could not be determined because they were simply too dense. The remarkable improvement in the conductivity observed with surfactant addition is attributed to the nanofibril-based network of the PEDOT phase.

In addition, a TEM study was conducted to investigate the morphology of PEDOT in pristine and surfactant-modified films of Clevios PH500 (see the SI, Figure S6). This returned results very similar to those of the Clevios P product, with the pristine film exhibiting granular PEDOT phases, whereas the surfactant-modified film had nanofibril PEDOT phases. It is believed that the surfactant provides these PEDOT chains with a sufficient increase in the chain mobility to facilitate their self-assembly into nanofibrils. On the basis of these results, a proposed morphology of the PEDOT:PSS thin film with Triton X-100 is illustrated in Figure 5e. The effect of diverse surfactants on the structure of PEDOT, focusing on the molecular weights of similar nonionic surfactants, should be further investigated in the future.

The $\pi-\pi$ stacking in the PEDOT phase was investigated by Raman spectroscopy, with Figure 6 showing the spectra of PEDOT:PSS films with and without surfactant. This demon-

dx.doi.org/10.1021/am500769k | ACS Appl. Mater. Interfaces 2014, 6, 6954−6961

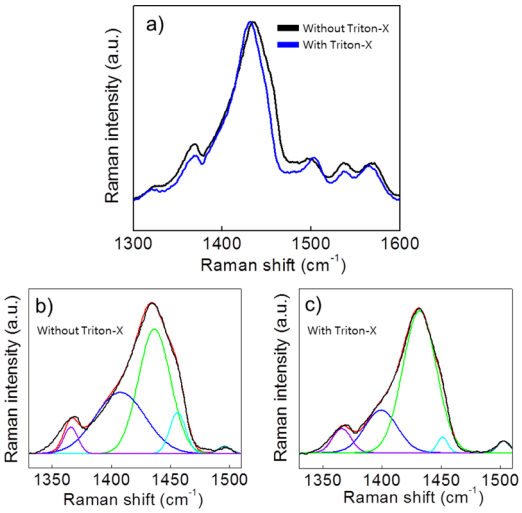

Figure 6. (a) Raman spectra for PEDOT:PSS films without/with surfactant. Deconvolution of the Raman spectra for PEDOT:PSS films (b) without and (c) with surfactant.

strates that the addition of surfactant shifts the main peak for PEDOT (1435 cm^{-1}) to a smaller wavenumber (1430 cm^{-1}), while the shoulder peak (1450 cm^{-1}) is also significantly reduced. This leftward shift of the main peak reflects a change in the resonance of PEDOT chains from a benzoic to quinoidal structure,[33] the latter preferring a planar geometry in the conjugated backbone that may provide better $\pi-\pi$ interaction, thereby facilitating one-dimensional growth.

To verify the coatability and enhanced conductivity by methanol washing, inverted organic solar cells with an active layer area of 5.4 mm^2 were fabricated from PEDOT:PSS films modified with Triton X-100 (f_{surf} = 1.0 wt %). The device was made by a consecutive coating: glass/ITO/ZnO/P3HT:ICBA/PEDOT:PSS. Note that the hydrophobic photoactive layer (P3HT:ICBA) prevents the use of pristine PEDOT:PSS films, while a glass substrate was used for the high annealing temperature (250 °C) required for a ZnO layer. Figure 7 shows

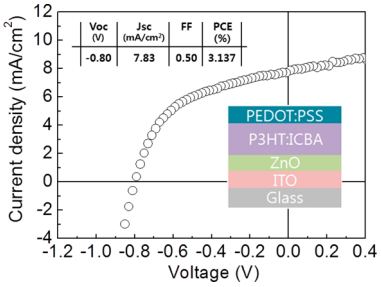

Figure 7. $J-V$ curves of inverted solar cells prepared using different PEDOT:PSS films with Triton X-100 (f_{surf} = 1.0 wt %) on a photoactive layer. Inset: Photovoltaic parameters and device structure.

the current density−voltage ($J-V$) curves of these inverted organic solar cells after partial washing of the PSS phase with methanol. This demonstrates that, without methanol washing, the power conversion efficiency (PCE) of the device was quite poor (see the SI, Figure S7), whereas after methanol washing, the $J-V$ curve was typical of polymer cells and the PCE value was increased to 3.14%. It is notable that a silver electrode was not used in this inverted cell and, instead, the enhanced conductivity afforded by methanol washing allowed PEDOT:PSS to function as the electrode.

It has been proven that the physical and electrical properties of nanofibril-based thin films are stable under large strains.[29,30] For example, poly(3-hexylthiophene) (P3HT) nanofibrils maintain the same conductivity, even at extreme strains,[31] which is attributed to the external strain being relieved by a straightening of the curved nanofibrils. The use of nanofibrils as active materials is therefore considered a promising option for the fabrication of highly flexible electronic devices. Figure 8a

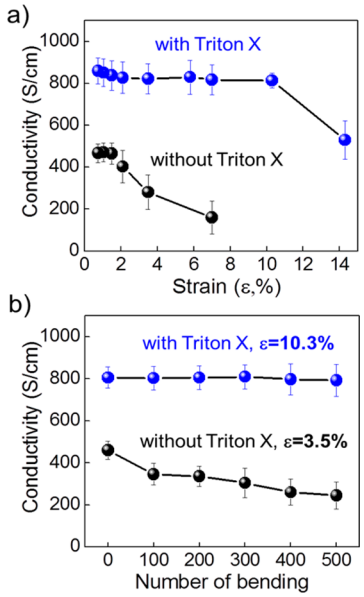

Figure 8. (a) Conductivity of the PEDOT:PSS thin films without/with surfactant as a function of the bending strain (ε). (b) Conductivity during repeated bending tests at ε = 10.3% for a thin film with surfactant and at ε = 3.5% for a thin film without surfactant.

shows the electrical conductivities of PEDOT:PSS films, both with and without Triton X-100, under increasing levels of strain. The 40-nm-thick films were spin-coated onto a 180-μm-thick PET substrate. The conductivity of the PEDOT:PSS film without surfactant was clearly stable at ∼430 S/cm when ε = 2.1% but was degraded to 160 S/cm at ε = 7.0%. On the other hand, the addition of surfactant (f_{surf} = 1.0 wt %) allowed the film to maintain its initial conductivity (∼830 S/cm), even under extreme strain (ε = 10.3%). The conductivity was reduced to 520 S/cm when a folded state was achieved (ε = 14.3%). Interestingly, the PEDOT:PSS films treated with polar solvents (DMSO and EG) did not show the same high flexibility. Instead, their conductivity was reduced from 650 S/cm at 2.1% strain to 363 S/cm at 7.0% strain (see the SI, Figure S8). This makes it clear that the network of PEDOT nanofibrils was responsible for enhancing the electrical stability to a greater extent than is possible with a network made of PEDOT granules. Figure 8b illustrates the change in the conductivity during repeated bending cycles. The film without Triton X-100 was performed at ε = 3.5%, whereas for the film with surfactant, it was carried out at ε = 10.3%. This demonstrates that the conductivity of a film without surfactant was gradually reduced at a relatively small strain as the number of bending cycles increased, whereas the conductivity of a PEDOT:PSS film with surfactant maintained its initial conductivity (∼830 S/cm) even at a higher strain level.

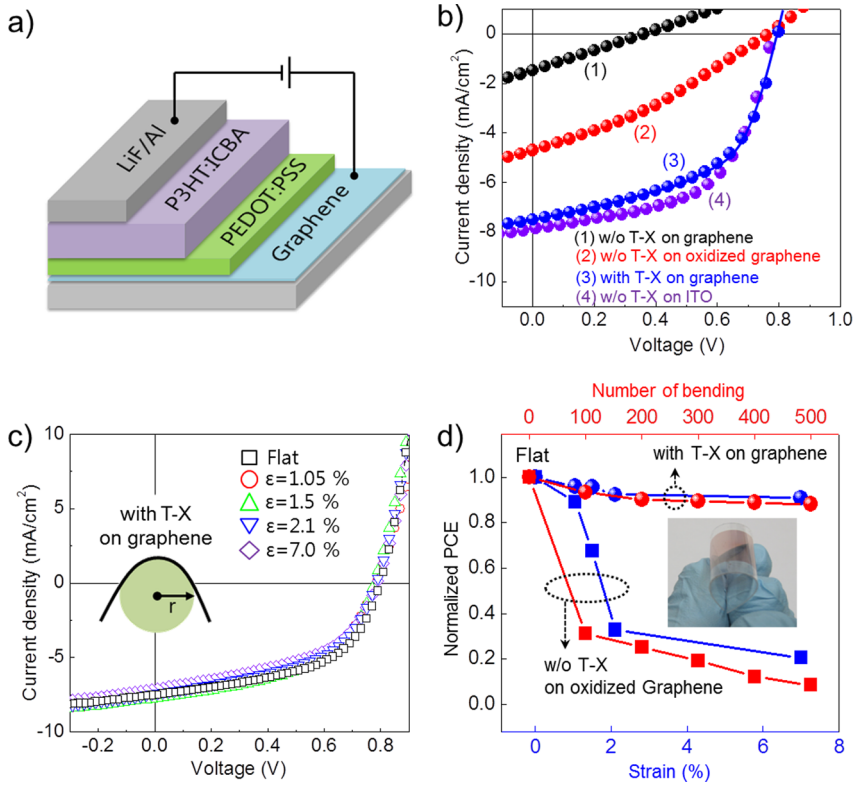

Figure 9. (a) Device structure of the P3HT:ICBA bulk-heterojunction solar cell fabricated in this study. (b) $J-V$ curves of the solar cells prepared using different electrodes without Triton X-100 on graphene, without Triton X-100 on oxidized graphene, with Triton X-100 on graphene, and without Triton X-100 on an ITO electrode. (c) $J-V$ curves of the solar cells prepared using the PEDOT:PSS film with surfactant (1.0 wt %) at different bending strains (□). (d) Blue symbols indicating normalized PCE of the solar cells prepared using PEDOT:PSS films without Triton X-100 on oxidized graphene (squares) and with Triton X-100 on graphene (circles) as a function of strain and red symbols showing normalized PCE during repeated bending tests at ε = 7.0%.

To take full advantage of the benefits of the PEDOT:PSS film developed, including its improved coatability on hydrophobic surfaces and its high conductivity, transparency, and stability under high strains, highly flexible organic solar cells were fabricated based on the structure depicted in Figure 9a. For this, PEDOT:PSS solutions were spin-coated onto bare graphene substrates (four graphene layers)/PET substrate, which were prepared by transferring a graphene layer synthesized by chemical vapor deposition (CVD) onto a PET substrate.[34,35] The optical transparency and sheet resistance of the graphene after annealing the PEDOT:PSS layer can be found in Figures S9 and S10, respectively, in the SI. The aim of inserting a graphene layer between the plastic substrate and PEDOT:PSS was for the passivation of water- and oxygen-containing gas molecules, which can improve the long-term device stability.[363738] To prevent crack propagation in the polymer photoactive layer under large strains, a bulk-heterojunction layer was employed that consisted of P3HT nanofibrils and indene-C_{60} bisadduct (ICBA) or phenyl-C_{61}-butyric acid methyl ester (PCBM). The preparation of this photoactive layer was accomplished using the procedure detailed in our previous report, in which a top electrode (LiF/Al, 0.8 nm/100 nm) was deposited on the photoactive layer by thermal evaporation under a high vacuum (10^{-6} Torr).

Figure 9b displays the $J-V$ curves obtained for each of the devices. Given that the pristine PEDOT:PSS was dewetted on a graphene substrate, it is not surprising that this device showed a poor PCE (η = 0.14%). When PEDOT:PSS was coated onto UVO-treated graphene, the PCE was increased to η = 1.153%. The increase in the sheet resistance of graphene (from 0.31 to 3.4 kΩ/□) conferred by UVO treatment reduced the current (J_{sc}). In comparison, PEDOT:PSS with surfactant (f_{surf} = 1.0 wt %) showed a greatly enhanced PCE (η = 3.14%) that was similar to the value achieved with an ITO/PET substrate (η = 3.47%). The related photovoltaic characteristics can be found in the SI (Table S1). The P3HT:PCBM solar cells all showed the same tendency with regard to PCE depending on the way in which the PEDOT:PSS/graphene hybrid electrodes were prepared (see the SI, Figure S11 and Table S2); the device fabricated from PEDOT:PSS with surfactant had a PCE of η = 2.55%. Figure 9c shows these PCE values of the P3HT:ICBA solar cell that was normalized to the strain applied to each device, with their accompanying photovoltaic characteristics summarized in the SI (Table S3). From this, it can be seen that, for a device fabricated using PEDOT:PSS with surfactant, 93% of the initial PCE value was retained at ε = 7.0%. Furthermore, this same device demonstrates excellent stability during repeated bending cycles at ε = 7.0% (red symbols in Figure 9d). In contrast, the device made of pristine PEDOT:PSS coated onto oxidized graphene retained only 21% of its initial PCE value at ε = 7.0% (see the SI, Figure S12). It is notable, however, that both devices were unstable at higher strain (i.e., folded) because of mechanical failure of the aluminum electrode.

CONCLUSION

Through this study, we have succeeded in producing a highly conductive PEDOT:PSS thin-film coating on hydrophobic

substrates, simply by adding a nonionic surfactant (Triton X-100) to an aqueous PEDOT:PSS solution. This surfactant was shown to significantly reduce the surface energy of the PEDOT:PSS solution, which is a key factor in enabling the coating of hydrophobic surfaces. Moreover, the surfactant resulted in the formation of PEDOT nanofibrils, with the conductive network they form leading to excellent electrical conductivity (830 S/cm) and low sheet resistance (250 Ω/□ at 96% transmittance at 550 nm). These nanofibrils also provided the PEDOT:PSS film with high electrical stability, even at extreme strain (ε = 10.3%). Full advantage was taken of the characteristics of the PEDOT:PSS film developed in this study to fabricate a highly flexible bulk-heterojunction polymer solar cell. A PEDOT:PSS/graphene hybrid electrode was used to mitigate the effects of humidity, resulting in a solar cell capable of maintaining its initial PCE (3.14%) under large strain (ε = 7.0%).

EXPERIMENTAL SECTION

Preparation of PEDOT. *PSS.* A PEDOT:PSS solution (Clevious P, Heraeus) containing 1.3 wt % solids was vigorously mixed with Triton X-100 (Aldrich) to a ratio of 1:2.5 by weight; i.e., the weight fraction (f_{surf}) of surfactant to PEDOT:PSS solute [f_{surf} = 100 (wt %) × W_{surf}/$W_{PEDOT:PSS}$] was 0.25−3 wt %. This mixed solution was spin-coated onto a diverse range of substrates, with the resulting films being thermally annealed at 140 °C for 10 min in air, and then washed with methanol.

Fabrication of a Multilayered Graphene Electrode. The graphene was synthesized by a CVD method, in which a copper foil catalyst was first inserted inside a quartz furnace tube and annealed at 1000 °C for 160 min under a 10 sccm flow of hydrogen gas (H_2). After annealing, 1 sccm of methane gas (CH_4) was injected to provide a carbon source for graphene synthesis, with the temperature being maintained for 5.5 h. Finally, the furnace was cooled to room temperature under a 10 sccm H_2 flow.

In order to fabricate a multilayered, stacked graphene electrode, the copper layer was wet-etched by a 0.1 M solution of ammonium persulfate and then transferred onto a PET substrate using poly(methyl methacrylate) (PMMA) as a supporting layer. Once the PMMA/graphene/PET sample was dry, the top layer of PMMA was removed with acetone. When this simple wet-transfer process was repeated, a multilayered graphene electrode was obtained. To provide a solar cell electrode, a 2.5 × 1 cm pattern was applied to graphene by a conventional patterning method.

Characterization. The surface tension of the PEDOT:PSS solutions was analyzed using an optical tensiometer (Biolin Scientific, Attension Theta Auto 3). The conductivity and sheet resistance of the films were measured with a four-point probe (CMT-SR1000N and MCP-T610), while their thickness was determined using an ellipsometer (Nano View, SE MG-1000 Vis) and a surface profiler (KLA-Tencor, AS 500). The morphology of the films was investigated by AFM (Digital Instrument, Nanoscope III) in tapping mode and TEM (JEOL JEM-2011HC) at 120 kV. A compositional analysis of the films was performed by XPS (Thermo, K-Alpha). Finally, the optical properties of the films were assessed with a Jasco V-650 spectrophotometer, and Raman spectra were obtained using a Raman spectrometer (Horriba Jovin Yvon, LabRam Aramis).

Fabrication and Characterization of Organic Solar Cells. To fabricate bulk-heterojunction solar cells, a PEDOT:PSS layer (40 nm) was first spin-coated onto a previously deposited graphene layer on a PET substrate and then annealed at 140 °C for 10 min in air. The electrode was then washed by dropping a few drops of methanol onto it while it was spun in the spin coater. After washing, the samples were dried at 100 °C for 10 min in a N_2 atmosphere. Photoactive solutions containing 2 wt % polymer (P3HT:ICBA, P3HT:PCBM dissolved in xylene, 1:1, w/w) were then spin-coated onto the PEDOT:PSS/graphene hybrid electrodes. To obtain a photoactive layer constructed from P3HT nanofibrils, the photoactive solution was first subjected to a cooling-and-heating process. Finally, a top electrode (LiF/Al, 0.8 nm/100 nm) was deposited onto all of the photoactive layers via thermal evaporation under high vacuum (low 10^{-6} Torr). The device area of the resulting solar cells was 5.4 mm^2. The photovoltaic characteristics of these devices were measured using a Keithley 2400 source measurement device under AM 1.5 solar illumination, with an irradiance of 100 mW/cm^2 generated using a 300 W Oriel solar simulator.

ASSOCIATED CONTENT

Supporting Information

Detailed experimental methods, AFM and TEM images of the PEDOT:PSS film, Raman, optical transmission, and XPS spectra of the PEDOT:PSS films, sheet resistance and electrical conductivity of the PEDOT:PSS film, and $J-V$ curves and a table of solar cells. This material is available free of charge via the Internet at http://pubs.acs.org.

AUTHOR INFORMATION

Corresponding Authors

*E-mail: thinfilm@yonsei.ac.kr.
*E-mail: ujeong@yonsei.ac.kr.

Notes

The authors declare no competing financial interest.

ACKNOWLEDGMENTS

This work was supported by a grant from the National Research Foundation of Korea (Grant 2012-0008721), funded by the Korean government (MEST). U.J. acknowledges financial support from the Samsung Research Funding Center of Samsung Electronics (Grant SRFC-MA1301-07).

REFERENCES

(1) Elschner, A. *PEDOT: Principles and Application of an Intrinsically Conducting Polymer*; Taylor & Francis Group: New York, 2011.
(2) Nardes, A. M.; Kemerink, M.; Janssen, R. A. J.; Bastiaansen, J. A. M.; Kiggen, N. M. M.; Langeveld, B. M. W.; Breemen, A. J. J. M. V.; Kok, M. M. D. Microscopic Understanding of the Anisotropic Conductivity of PEDOT:PSS Thin Films. *Adv. Mater.* **2007**, *19*, 1196−1200.
(3) Lang, U.; Müller, E.; Naujoks, N.; Dual, J. Microscopical Investigations of PEDOT:PSS Thin Films. *Adv. Funct. Mater.* **2009**, *19*, 1215−1220.
(4) Günes, S.; Neugebauer, H.; Sariciftci, N. S. Conjugated Polymer-Based Organic Solar Cells. *Chem. Rev.* **2007**, *107*, 1324−1338.
(5) Groenendaal, L.; Jonas, F.; Freitag, D.; Pielartzik, H.; Reynolds, J. R. Poly(3,4-ethylenedioxythiophene) and Its Derivatives: Past, Present, and Future. *Adv. Mater.* **2000**, *12*, 481−494.
(6) Crispin, X.; Jakobsson, F. L. E.; Crispin, A.; Grim, P. C. M.; Andersson, P.; Volodin, A.; Haesendonck, C. V.; Auweraer, M. V. D.; Salaneck, W. R.; Berggren, M. The Origin of the High Conductivity of Poly(3,4-ethylenedioxythiophene)−Poly(styrenesulfonate) (PEDOT−PSS) Plastic Electrodes. *Chem. Mater.* **2006**, *18*, 4354−4360.
(7) Park, H.; Chang, S.; Smith, M.; Gradecak, S.; Kong, J. Interface Engineering of Graphene for Universal Applications as Both Anode and Cathode in Organic Photovoltaics. *Sci. Rep.* **2013**, *3*, 1581.
(8) Park, H.; Shi, Y.; Kong, J. Application of Solvent Modified PEDOT:PSS to Graphene Electrodes in Organic Solar Cells. *Nanoscale* **2013**, *5*, 8934−8939.
(9) Cho, C.-K.; Hwang, W.-J.; Eun, K.; Choa, S.-H.; Na, S.-I.; Kim, H.-K. Mechanical Flexibility of Transparent PEDOT:PSS Electrodes Prepared by Gravure Printing for Flexible Organic Solar Cells. *Sol. Energy Mater. Sol. Cells* **2011**, *95*, 3269−3275.

(10) Kawano, K.; Pacious, R.; Poplavskyy, D.; Nelson, J.; Bradley, D. D. C.; Durrant, J. R. Degradation of Organic Solar Cells Due to Air Exposure. *Sol. Energy Mater. Sol. Cells* **2006**, *90*, 3520−3530.
(11) Lee, J.-H; Shin, H.-S.; Na, S.-I.; Kim, H.-K. Transparent and Flexible PEDOT:PSS Electrodes Passivated by Thin IZTO Film Using Plasma-Damage Free Linear Facing Target Sputtering for Flexible Organic Solar Cells. *Sol. Energy Mater. Sol. Cells* **2013**, *109*, 192−198.
(12) Hau, S. K.; Yip, H.-L.; Baek, N. S.; Zou, J.; Omalley, K.; Jen, A. K.-Y. High Performance Ambient Processed Inverted Polymer Solar Cells Through Interfacial Modification with a Fullerene Self-Assembled Monolayer. *Appl. Phys. Lett.* **2008**, *92*, 253301.
(13) Na, S.-I.; Wang, G.; Kim, S.-S.; Kim, T.-W.; Oh, S.-H.; Yu, B.-K.; Lee, T.; Kim, D.-Y. Evolution of Nanomorphology and Anisotropic Conductivity in Solvent-Modified PEDOT:PSS Films for Polymeric Anodes of Polymer Solar Cells. *J. Mater. Chem.* **2009**, *19*, 9045−9053.
(14) Ouyang, J.; Xu, Q.; Chu, C.-W.; Yang, Y.; Li, G.; Shinar, J. On the Mechanism of Conductivity Enhancement in Poly(3,4-ethylenedioxythiophene):poly(styrene sulfonate) Film through Solvent Treatment. *Polymer* **2004**, *45*, 8443−8450.
(15) Kim, Y. H.; Sachse, C.; Machala, M. L.; May, C.; Muller-Meskamp, L.; Leo, K. Highly Conductive PEDOT:PSS Electrode with Optimized Solvent and Thermal Post-Treatment for ITO-Free Organic Solar Cells. *Adv. Funct. Mater.* **2011**, *21*, 1076−1081.
(16) Crispin, X.; Jakobsson, F. L. E.; Crispin, A.; Grim, P. C. M.; Andersson, P.; Volodin, A.; van Haesendonck, C.; Van der Auweraer, M.; Salaneck, W. R.; Berggren, M. The Origin of the High Conductivity of Poly(3,4-ethylenedioxythiophene)−Poly-(styrenesulfonate) (PEDOT−PSS) Plastic Electrodes. *Chem. Mater.* **2006**, *18*, 4354−4360.
(17) Nardes, A. M.; Kemerink, M.; de Kok, M. M.; Vinken, E.; Maturova, K.; Janssen, R. A. J. Conductivity, Work Function, and Environmental Stability of PEDOT:PSS Thin Films Treated with Sorbitol. *Org. Electron.* **2008**, *9*, 727−734.
(18) Po, R.; Carbonera, C.; Bernardi, A.; Tinti, F.; Camaioni, N. Polymer- and Carbon-Based Electrodes for Polymer Solar Cells: Toward Low-Cost, Continuous Fabrication over Large Area. *Sol. Energy Mater. Sol. Cells* **2012**, *100*, 97−114.
(19) Xia, Y.; Sun, K.; Ouyang, J. Solution-Processed Metallic Conducting Polymer Films as Transparent Electrode of Optoelectronic Devices. *Adv. Mater.* **2012**, *24*, 2436−2440.
(20) Kim, N.; Kee, S.; Lee, S. H.; Lee, B. H.; Kahng, Y. H.; Jo, Y.-R.; Kim, B.-J.; Lee, K. Highly Conductive PEDOT:PSS Nanofibrils Induced by Solution-Processed Crystallization. *Adv. Mater.* **2014**, *26*, 2268−2272.
(21) Fabretto, M. V.; Evans, D. R.; Mueller, M.; Zuber, K.; Hojati-Talemi, P.; Short, R. D.; Wallace, G. G.; Murphy, P. J. Polymeric Material with Metal-Like Conductivity for Next Generation Organic Electronic Devices. *Chem. Mater.* **2012**, *24*, 3998−4003.
(22) Bolognesi, M.; Sanchez-Diaz, A.; Ajuria, J.; Pacios, R.; Palomares, E. The Effect of Delective Contact Electrodes on the Interfacial Charge Recombination Kinetics and Device Efficiency of Organic Polymer Solar Cells. *Phys. Chem. Chem. Phys.* **2011**, *13*, 6105−6109.
(23) Vosgueritchian, M.; Lipomi, D. J.; Bao, Z. Highly Conductive and Transparent PEDOT:PSS Films with a Fluorosurfactant for Stretchable and Flexible Transparent Electrodes. *Adv. Funct. Mater.* **2012**, *22*, 421−428.
(24) Lang, U.; Naujoks, N.; Dual, J. Mechanical Characterization of PEDOT:PSS Thin Films. *Synth. Met.* **2009**, *159*, 473−479.
(25) Lee, Y.-Y.; Lee, J.-H.; Cho, J.-Y.; Kim, N.-R.; Nam, D.-H.; Chio, I.-S.; Nam, K. T.; Joo, Y.-C. Stretching-Induced Growth of PEDOT-Rich Cores: A New Mechanism for Strain-Dependent Resistivity Change in PEDOT:PSS Films. *Adv. Funct. Mater.* **2013**, *23*, 4020−4027.
(26) Takano, T.; Masunaga, H.; Fujiwara, A.; Okuzaki, H.; Sasaki, T. PEDOT Nanocrystal in Highly Conductive PEDOT:PSS Polymer Films. *Macromolecules* **2012**, *45*, 3859−3865.
(27) Hu, T.; Shklovskii, B. I. Theory of Hopping Conductivity of a Suspension of Nanowires in an Insulator. *Phys. Rev. B* **2006**, *74*, 054205.
(28) Hu, L.; Hecht, D. S.; Grüner, G. Percolation in Transparent and Conducting Carbon Nanotube Networks. *Nano Lett.* **2004**, *4*, 2513−2517.
(29) McCardle, R.; Fakirov, S.; Bhattacharyya, D. Nanofibrillar Polymer−Polymer Composites: Effect of Reinforcement Orientation on the Mechanical Properties. *Macromol. Symp.* **2013**, *327*, 64−71.
(30) Duhovic, M.; Bhattacharray, D.; Fakirov, S. Nanofibrillar Single Polymer Composites of Poly(ethylene terephthalate). *Macromol. Mater. Eng.* **2010**, *295*, 95−99.
(31) Oh, J. Y.; Shin, M.; Lee, T. I.; Jang, W. S.; Lee, Y.-J.; Kim, C. S.; Kang, J.-W.; Myoung, J.-M.; Baik, H. K.; Jeong, U. Highly Bendable Large-Area Printed Bulk Heterojunction Film Prepared by the Self-Seeded Growth of Poly(3-hexylthiophene) Nanofibrils. *Macromolecules* **2013**, *46*, 3534−3543.
(32) Vosgueritchian, M.; Lipomi, D. J.; Bao, Z. Highly Conductive and Transparent PEDOT:PSS Films with a Fluorosurfactant for Stretchable and Flexible Transparent Electrodes. *Adv. Funct. Mater.* **2012**, *22*, 421−428.
(33) Ouyang, J.; Chu, C.-W.; Chen, F.-C.; Xu, Q.; Yang, Y. High-Conductivity Poly(3,4-ethylenedioxythiophene):Poly(styrene sulfonate) Film and Its Application in Polymer Optoelectronic Devices. *Adv. Funct. Mater.* **2005**, *15*, 203−208.
(34) Kim, K. S.; Zhao, Y.; Jang, H.; Lee, S. Y.; Kim, J. M.; Kim, K. S.; Ahn, J.-H.; Kim, P.; Choi, J.-Y.; Hong, B. H. Large-Scale Pattern Growth of Graphene Films for Stretchable Transparent Electrodes. *Nature* **2009**, *457*, 706−710.
(35) Bae, S.; Kim, H.; Lee, Y.; Xu, X.; Park, J.-S.; Zheng, Y.; Balakrishnan, J.; Lei, T.; Kim, H. R.; Song, Y. I.; Kim, Y.-J.; Kim, K. S.; Özyilmaz, B.; Ahn, J.-H.; Hong, B. H.; Iijima, S. Roll-to-Roll Production of 30-Inch Graphene Films for Transparent Electrodes. *Nat. Nanotechnol.* **2010**, *5*, 574−578.
(36) Oh, J. Y.; Lee, T. I.; Myoung, J. M.; Jeong, U.; Baik, H. K. Coating on a Cold Substrate Largely Enhances Power Conversion Efficiency of the Bulk Heterojunction Solar Cell. *Macromol. Rapid Commun.* **2011**, *32*, 1066−1071.
(37) Oh, J. Y.; Shin, M.; Lee, T. I.; Jang, W. S.; Min, Y.; Myoung, J. M.; Baik, H. K.; Jeong, U. Self-Seeded Growth of Poly(3-hexylthiophene) (P3HT) Nanofibrils by a Cycle of Cooling and Heating in Solutions. *Macromolecules* **2012**, *45*, 7504−7513.
(38) Oh, J. Y.; Lee, T. I.; Jang, W. S.; Chae, S. S.; Park, J. H.; Lee, H. W.; Myoung, J.-M.; Baik, H. K. Mass Production of a 3D Non-Woven Nanofabric with Crystalline P3HT Nanofibrils for Organic Solar Cells. *Energy Environ. Sci.* **2013**, *6*, 910−917.